Application of a Fully 3D Printed Carbon Electrode for the Double Potential Step Chronocoulometric Determination of 2,4dinitrophenol in Environmental Water Samples

Daniel Steven Shaw , Zuhayr Rymansaib , Pejman Iravani , Kevin C. Honeychurch *

Posted Date: 8 May 2025

doi: 10.20944/preprints202505.0594.v1

Keywords: 3D printed electrode; Carbon nanofiber; Chronocoulometry; 2,4-dinitrophenol; Environmental water sample

Article

Application of a Fully 3D Printed Carbon Electrode for the Double Potential Step Chronoamperometry Determination of 2,4-dinitrophenol in Environmental Water Samples

Daniel Steven Shaw [1,2], Zuhayr Rymansaib [3], Pejman Iravani [3] and Kevin C. Honeychurch [4,*]

[1] Institute of Bio-Sensing Technology, University of the West of England, Frenchay Campus, Coldharbour Lane, Bristol BS16 1QY, UK

[2] Department of High-Capacity Diagnostics, Statens Serum Institut, 2300 Copenhagen, Denmark

[3] Department of Mechanical Engineering, University of Bath, Claverton Down, Bath BA2 7AY, UK

[4] Centre for Biomedical Research (CBR), School of Applied Sciences, University of the West of England, Frenchay Campus, Coldharbour Lane, Bristol BS16 1QY, UK

* Correspondence: kevin.honeychurch@uwe.ac.uk

Abstract: This paper demonstrates the first reported application of a fully 3D printed carbon nanofiber–graphite–polystyrene working electrode for the double potential step chronoamperometric determination of 2,4-dinitrophenol in an environmental water sample. Initial cyclic voltammetric investigations were undertaken to characterise the redox behaviour of 2,4-dinitrophenol over the pH range 2 to 8. During the initial negative scan, two reduction peaks were observed, attributed to the reduction of the two nitro groups to their respective hydroxylamines. On the subsequent positive scan, two oxidation peaks were detected, corresponding to the oxidation of the hydroxylamines formed during the initial negative scan. All peaks were found to be pH dependent over the range studied. Using a double potential step chronoamperometric approach (step 1 = -1.4 V; step 2 = +0.8 V), a calibration plot was constructed and found to be linear from 50 μM to 1.0 mM (R^2= 0.9978) with a detection limit of 7.8 μM (based on a signal-to-noise ratio of 3). The method was evaluated by carrying out 2,4-dinitrophenol determinations on a fortified and unfortified environmental pond water sample. Using external calibration, a mean recovery of 106 % was obtained with an associated coefficient of variation of 3.6 % calculated for a concentration of 50 μM. The results show that these 3D printed electrodes are a promising alternative to electrodes fabricated using traditional materials and that reliable data may be obtained for 2,4-dinitrophenol in environmental water samples.

Keywords: 3D printed electrode; carbon nanofiber; chronoamperometry; 2,4-dinitrophenol; environmental water sample

1. Introduction

Nitrophenols are aromatic organic compounds consisting of benzene rings, and nitro (-NO_2) and hydroxyl (-OH) groups. The phenolic compound 2,4-dinitrophenol (2,4-DNP) has been used in the manufacture of industrial products, such as dyes, pharmaceuticals, pesticides, wood preservatives, and even in explosives with military applications. It can enter surface waters with effluents from these industries or through the use of pesticides. The accumulation of 2,4-DNP in environmental water [1] and air [2] has led to the classification of 2,4-DNP as a priority pollutant by the US Environmental Protection Agency [3]. Some studies have stated its concentration in industrial effluent is around 1000 mg/L [4,5]. The release of industrial effluent, wastewater, or pesticides containing 2,4-DNP into the receiving water poses a direct and significant hazard to the ecosystem and public health.

The effects of nitrophenols on aquatic biota are well-documented. Exposure of fish to 2,4-DNP has been reported to negatively affect swimming performance [6] as well as nervous, endocrine,

 doi:10.20944/preprints202505.0594.v1

reproductive, and digestive systems [7]. The median lethal concentration (LC_{50}) of 2,4-DNP varies depending on taxonomy of the organism; the LC_{50} of 2,4-DNP for freshwater algae is much higher than that of freshwater fish for example. Toxicity to plants has also been recorded in a range of studies [8] with 2,4-DNP reported to interfere with metabolic processes such as respiration and photosynthesis, and affect seed germination rates [9,10], root development [11,12], and numerous other processes.

Studies on the absorption, distribution, metabolism, and excretion of 2,4-DNP have been performed mainly in laboratory specimens, but some information about the levels of the drug and its metabolites in humans is available from cases of occupational intoxications or ingestion of diet pills. One of the first reports of occupational intoxication with 2,4-DNP relates to the filling of armour-piercing shells with a mixture of dinitrophenol and picric acid [13] during the First World War. French munition workers during the war reported problems associated with exposure to 2,4-DNP with symptoms of weight loss, weakness, dizziness, sweating, and even death by hyperthermia [13,14]. Subsequent investigations showed that exposure to 2,4-DNP caused these symptoms [15]. It does so by acting as a protonophore and dissipating the proton gradient across the mitochondrial membrane. This disrupts the proton motive force that the cell uses to synthesise the majority of its adenosine triphosphate (ATP) used to store chemical energy. The inefficiency is proportional to the dose of 2,4-DNP that is taken and results in heat generation and calorie consumption. The noted calorie consumption and subsequent weight loss led to 2,4-DNP being used as a dieting aid in the 1930s with adverse reports appearing soon afterwards [16]. Consequently, it was banned for human consumption in the UK, USA, and elsewhere. However, 2,4-DNP has recently been marketed as a dieting aid, principally via unregulated sales on the internet which has resulted in reports of toxicity incidents and a number of deaths [17–22]. A lethal oral dose of 2,4-DNP for a human is typically considered to be 14 to 43 mg/kg of bodyweight [23]. Nevertheless, a number of recent studies have shown that mild mitochondrial uncoupling induced by the controlled application of low-dose 2,4-DNP may have clinical applications in the treatment of neurodegenerative conditions [24–26], diabetes, and steatohepatitis [27]. To ensure public health security and environmental protection, there is a need for analytical techniques capable of determining 2,4-DNP in complex samples such as environmental water.

Nitro-aromatic compounds are known to exhibit a range of interesting electrochemical behaviours [28–31]. The methods used to determine these compounds are mainly based on gas chromatography [32] high-performance liquid chromatography [33,34] and liquid chromatography coupled with mass spectrometry [35]. These methods, while accurate, often have long analysis times and high running costs. Consequently, increasing attention has been paid to electrochemical methods, because of their rapid operation and inexpensive instrumentation. In previous studies, we have shown the voltammetric behaviour of 2,4-DNP at a glassy carbon electrode [31] and its determination in serum by differential pulse voltammetry. Investigations showed that the nitro groups of 2,4-DNP can be reduced to the corresponding hydroxylamine which can be subsequently oxidised to a nitroso species. This offers a number of advantages and possibilities for the analytical determination of 2,4-DNP.

In recent years, three-dimensional (3D) printing has moved beyond its original application of industrial manufacturing and prototyping to much wider fields, including the fabrication of both physical and chemical sensors [36–39]. 3D printing allows for the simple fabrication of new composite designs and other important sensor components such as micro-fluidic sample handling systems [36], analyte accumulation layers [40], and even whole electrochemical cells [36]. The possibility of fabricating these with high precision using robotic printing techniques has also been demonstrated [41]. Further advantages can be seen from the considerable percentage of 3D printing technology available via the open-source model; allowing the advantages of creative adaption of methods and for open sharing of expertise and innovation [42]. Studies have shown the possibility of using the technology to fabricate carbon electrodes [43–53], offering an attractive alternative to other carbon electrode fabrication techniques, such as screen printing and carbon paste, and an alternative to the use of expensive electrode materials, such as glassy carbon. Recently, Silva et al. [51] have discussed the development of tailored filaments composed of reduced graphene oxide (rGO) and carbon black

 doi:10.20944/preprints202505.0594.v1

(CB) in a polylactic acid (PLA) matrix for the production of 3D-printed electrochemical sensors. Electrodes containing rGO were found to show improved performance, with improved conductivity and lower charge transfer resistance. The developed electrodes were applied to the detection of 2,4,6-trinitrotoluene (TNT) and cocaine; giving a limit of detection of 0.33 μM for TNT. A graphite/alumina/polylactic acid (G/Al_2O_3/PLA)-based 3D-printed electrode for the electrochemical determination of TNT has also been described by Brum et al. [52]. The possibility of using square wave voltammetry to determine TNT residues at this electrode in samples of tap water, lagoon, and seawater was explored. Recoveries of between 100-106% were reported, and the possibility of using this electrode for detecting TNT residues present on different surfaces was shown to allow for ng levels to be determined. The possibility of determining TNT in environmental samples has also recently been investigated at a 3D-printed microfluidic chip by Wang et al. [53]. This incorporated a TNT biosensing complex and was reported to give a linear relationship for TNT over the range of 0.1–100 μg/mL with a LOQ of 0.81 μg/mL

However, the majority of 3D printed electrodes generally require further modification and only use 3D printing to produce the base structure. Recently, it has been shown possible to fully fabricate carbon electrodes using 3D printing alone, without the need for further fabrication steps [49]. The determination of Pb [49] and Zn [45] at these electrodes fabricated from 3D printed carbon nanofiber–graphite–polystyrene has been demonstrated and we believe it is possible to determine other compounds using these same electrodes. In this present study, we investigated the cyclic voltammetric behaviour of 2,4-DNP at a fully 3D printed carbon nanofiber–graphite–polystyrene working electrode. We then explored the possibility of determining 2,4-DNP by chronoamperometry in an environmental water sample.

2. Materials and Methods

2.1. Chemicals and Reagents

Unless otherwise specified, all chemicals were sourced from Fisher Scientific (Loughborough, UK). Deionised water was produced using a Purite RO200-Stillplus HP System (Purite Water Purification Solutions, Oxon, UK). Stock solutions of orthophosphate were prepared at a concentration of 0.2 M by dissolving the appropriate mass in deionised water. These solutions were then titrated together to achieve the desired pH. Stock solutions of 2,4-DNP were prepared by dissolving the required amount in acetonitrile to achieve a concentration of 10 mM. Working standards for voltammetric and chronoamperometric studies were prepared by diluting the primary stock solution with phosphate buffer and acetonitrile to achieve a final solution of 0.1 M phosphate buffer,10% acetonitrile.2.2 Apparatus

Cyclic voltammetry and chronoamperometry were undertaken using an EmStat3 potentiostat (Ivium Technologies, Eindhoven, the Netherlands) interfaced to a PC for instrument control and data acquisition. The voltammetric cell contained a carbon rod auxiliary electrode, a Ag/AgCl/KCl(3M) reference electrode, and a 3D printed carbon nanofiber–graphite–polystyrene electrode as the working electrode. The 3D printed carbon electrode was rinsed with deionised water, polished with tissue paper, rinsed a second time in deionised water, and dried under a stream of nitrogen gas before each scan.

2.3. Cyclic Voltammetry

Cyclic voltammograms were recorded with solutions of 0.1 M phosphate buffer containing 10 % acetonitrile, and then in the same solution containing 1.0 mM 2,4-DNP. Samples were purged with nitrogen gas (BOC, Guildford, UK) for 5 minutes to remove dissolved oxygen. Cyclic voltammetric investigations were undertaken using either (i) a starting and end potential of 0.0 V, an initial switching potential of -1.5 V, and a second switching potential of +1.0 V, or (ii) a starting and end potential of 0.0 V, an initial switching potential of +1.0 V, and a second switching potential of -1.5 V.

 doi:10.20944/preprints202505.0594.v1

2.4. Double Potential Step Chronoamperometry

Double potential step chronoamperometric studies were undertaken in solutions of 0.1 M pH 2.0 phosphate buffer, containing 10 % acetonitrile using the potential waveform shown in Scheme 1. Step 1: applied potential at -1.4 V for 60 s. Step 2: applied potential of +0.8 V for 60 s.

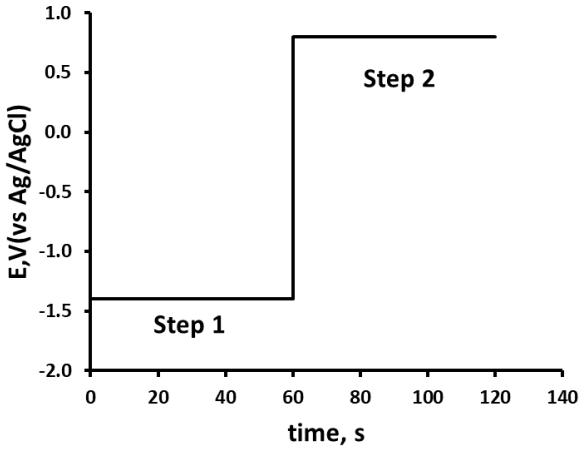

Scheme 1. Potential waveform for double potential step chronoamperometry. Step 1, -1.4 V from 0 to 60 s; Step 2, 0.8 V 60 to 120 s.

2.5. Fabrication of Electrodes

2.5.1. Composite Thermoplastic Filament Fabrication

The procedure for the preparation of the composite thermoplastic filament has been published previously [49]. To fabricate a total of 5 g of electrode material, 4 g of polystyrene (Sigma-Aldrich, Germany) were dissolved in 50 mL of chloroform. Separately, 0.5 g of carbon nanofibers (PR 24 XT HHT) and 0.5 g of graphite flakes (Sigma Aldrich, Germany) were sonicated in 50 mL of chloroform for 20 minutes. The resulting two mixtures were added to an open container and heated on a magnetic stirrer at 50 °C in a fume cupboard until the solvent fully evaporated. Once the solvent had completely evaporated, the resulting solid thermoplastic composite was placed in a heated at 220 °C in a 2 mm internal diameter aluminium barrel and extruded into lengths of composite conductive filament for 3D printing.

2.5.2. Computer-Aided Design and 3D Printing

CAD software Solid Edge ST6 was used to design the electrode as a multi-material component; with an electrode tip of 4.5 mm by 7.5 mm, with a central active area of 0.656 mm². Printing commands were generated from the CAD file using the open-source software Slic3r (available at slic3r.org). A layer height of 350 μm was used, resulting in 9 layers for the complete electrode. The electrodes were printed using a custom-built fused filament deposition 3D printer with two 0.5 mm extruders.2.6 Analytical application

Environmental pond water samples were collected from Frenchay Campus, University of the West of England, Bristol, UK (51° 29' 55.6" N 2° 32' 40.5" W). A 4.0 mL aliquot of the environmental water sample was diluted to be 10 % acetonitrile in 0.1 M phosphate buffer pH 2.0. A second aliquot of the environmental water sample was fortified to give 50 μM 2,4-DNP, and then diluted tenfold to give a 10 % acetonitrile and 0.1 M phosphate buffer pH 2.0 solution. These were examined using the optimised double potential step chronoamperometric procedure.

 doi:10.20944/preprints202505.0594.v1

3. Results and Discussion

3.1. Cyclic Voltammetry

The cyclic voltammetric behaviour of 2,4-DNP was studied over the range pH 2 to pH 8 (representative voltammograms obtained at pH 2 shown in Figure 1). Using an initial negative-going scan, two reduction peaks were recorded and designated R1 and R2. These are thought to result from the reduction of the two nitro groups to their corresponding hydroxylamines (Equation 1). On the subsequent positive-going scan, two oxidation peaks are observable (designated O1 and O2) corresponding to the oxidation of the electrochemically-generated hydroxylamine to the corresponding nitrosamine (Equation 2).

$$R\text{-}NO_2 + 4e^- + 4H^+ \rightarrow R\text{-}N(H)\text{-}OH + H_2O \quad (1)$$

$$R\text{-}N(H)\text{-}OH \rightarrow R\text{-}N{=}O + 2e^- + 2H^+ \quad (2)$$

Further studies were undertaken to investigate this proposed mechanism. If the voltammetric scan was first implemented in a positive direction, no oxidation peaks were observable. Thus, the oxidative responses did not occur unless the molecule had undergone some previous reduction process. Hence, it was concluded that the two oxidation peaks result from the oxidation of the hydroxylamine (Equation 2) formed via the process described in Equation 1.

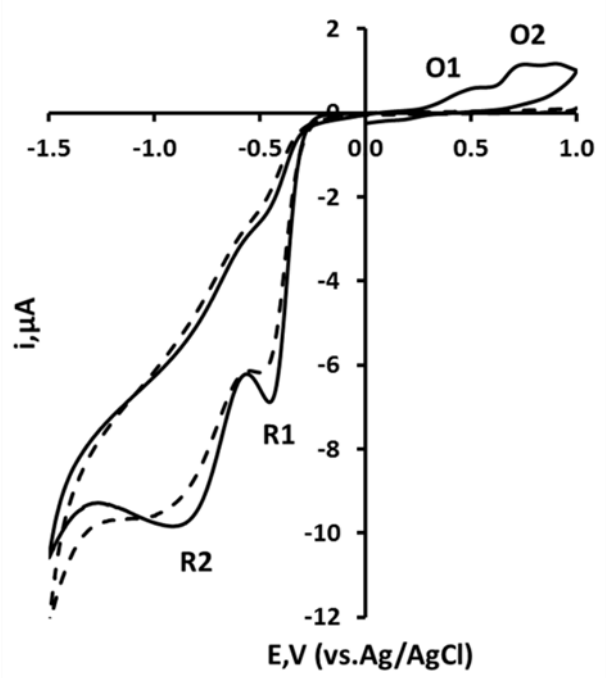

Figure 1. Cyclic voltammograms recorded at a 3D printed carbon nanofiber–graphite–polystyrene electrode for a 1.0 mM solution of 2,4-dinitrophenol in 10% acetonitrile, buffered with 100 mM phosphate at pH 2 at a scan rate of 50 mV/s for solid line: Starting and ending potential at 0.0 V, initial switching potential at -1.5 V, and second switching potential at +1.0 V. Dashed line: Starting and ending potential at 0.0 V, initial switching potential at +1.0 V, and second switching potential at -1.5 V.

3.2. Effect of pH on Peak Potential

The peak potential (Ep) for peaks R1, R2, O1, and O2 was obtained over the range pH 2–8 (Figure 2). All of the peaks observed were found to be pH dependent. Plots of the Ep values of peaks R1, R2, and O2 against pH were found to give slope close the Nernst theoretical values of 59 mV/pH indicating an equal number of protons and electrons were involved in their reductions or oxidations. However, peak O1 was found to have a break point at pH 4.1. It is possible that this is a result of acid

 doi:10.20944/preprints202505.0594.v1

dissociation (pKa) associated with the phenol group. The pKa of 2,4-dinitrophenol is 4.13 [54], which is close to the result obtained. Consequently, we believe that oxidation process seen at O1 is related to the oxidation of the phenolic group. However, this oxidation is not observable with prior reduction of the molecule and is, presumably, a result of an inductive effect on the hydroxylamine oxidation. The possibility of direct electrochemical oxidation of 2,4-DNP via one-electron oxidation of the phenolic group has been demonstrated previously [55]. However, we have not seen evidence for this in the cyclic voltammetric investigation conducted here.

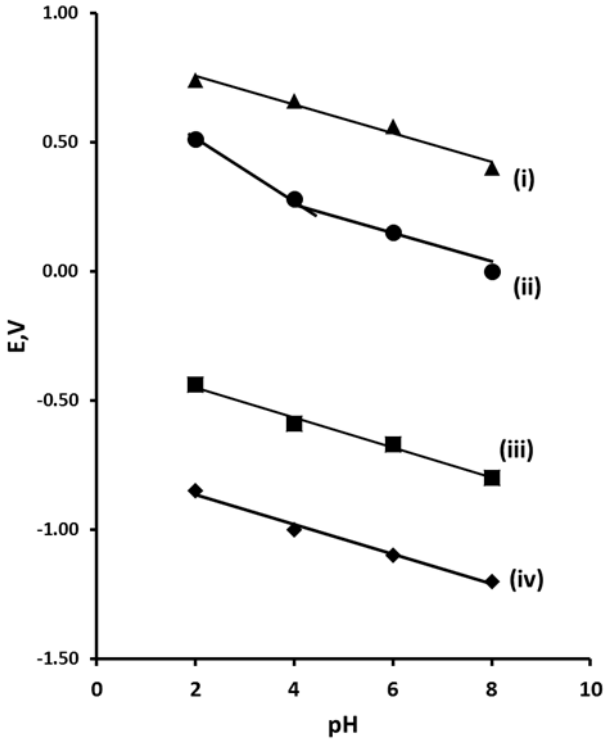

Figure 2. Plot of Ep vs. pH for 2,4-dinitrophenol. (i) peak O2, (ii) peak O1, (iii) peak R1, (iv) peak R2.

3.3. Double Potential Step Chronoamperometry

Chronoamperometry offers the possibility of simple operation and utility outside of the laboratory with small sample volumes. In comparison to other amperometric techniques, chronoamperometry can give an improved signal-to-noise ratio as the current can be integrated over longer time intervals. As we were interested in determining low concentrations of 2,4-DNP, we chose to investigate the possibility of utilising a chronoamperometric measure step for the determination of 2,4-DNP. We focused our investigations on the anodic oxidation of the electrochemically generated hydroxylamine species (Equation 2). This offers analytical advantages, as it avoids interference from the reduction of sample components, such as oxygen and common metal ions.

We first investigated the chronoamperometric behaviour of a quiescent 10 % acetonitrile 0.1 M pH 2 phosphate buffer in the presence and absence of 1 mM 2,4-DNP. A potential of -1.4 V was applied for 30 s to reduce 2,4-DNP to its corresponding hydroxylamine (Equation 1). The potential was step to +1.0 V and held for 60 s to oxidise the hydroxylamine formed to the nitrosamine, giving the analytical signal (Figure 3a). Plots of current (i) vs. the inverse of the square root of time ($t^{-½}$) showed the response to follow Cottrell type behaviour (Figure 3b) [56].

 doi:10.20944/preprints202505.0594.v1

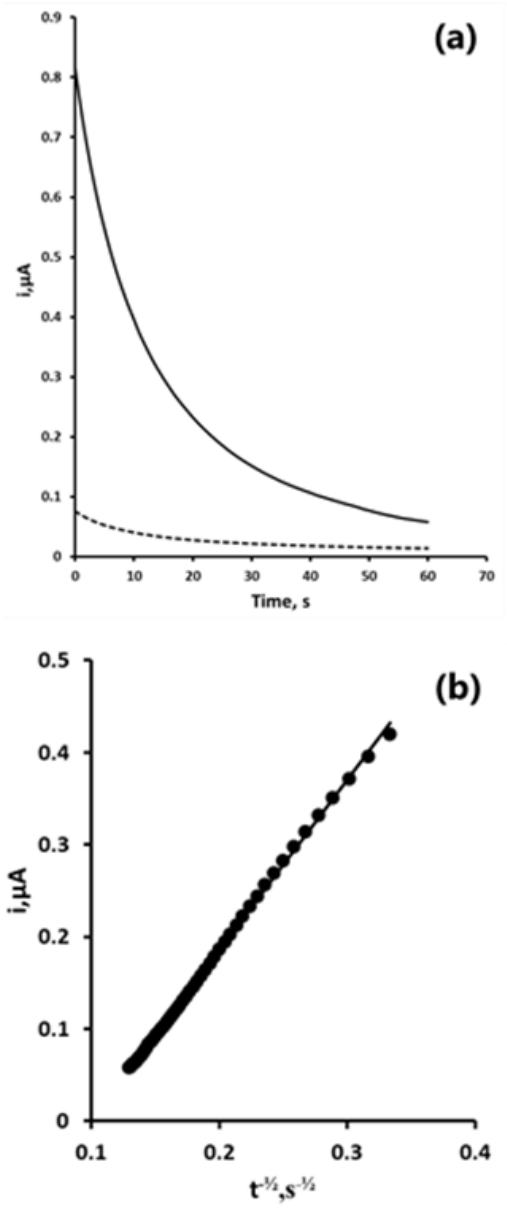

Figure 3. (a) Chronoamperometric response obtained in the presence (solid line) and absence (dashed line) of 1 mM 2,4-DNP; (b) Cottrell plot of 1 mM 2,4-DNP obtained from the chronoamperometric response (a).

3.4. The Effect of pH on the Chronoamperometric Response

The chronoamperometric current response was found to be pH dependent over the range studied (Figure 4) and was found to decrease with increasing pH. This was likely due to the stabilisation of the nitro groups of 2,4-DNP by the phenolate anion. The maximum peak current of the oxidation peak O1 was on found at pH 2.0. Therefore, subsequent studies were undertaken using a supporting electrolyte of 0.1 M pH 2.0 phosphate buffer.

 doi:10.20944/preprints202505.0594.v1

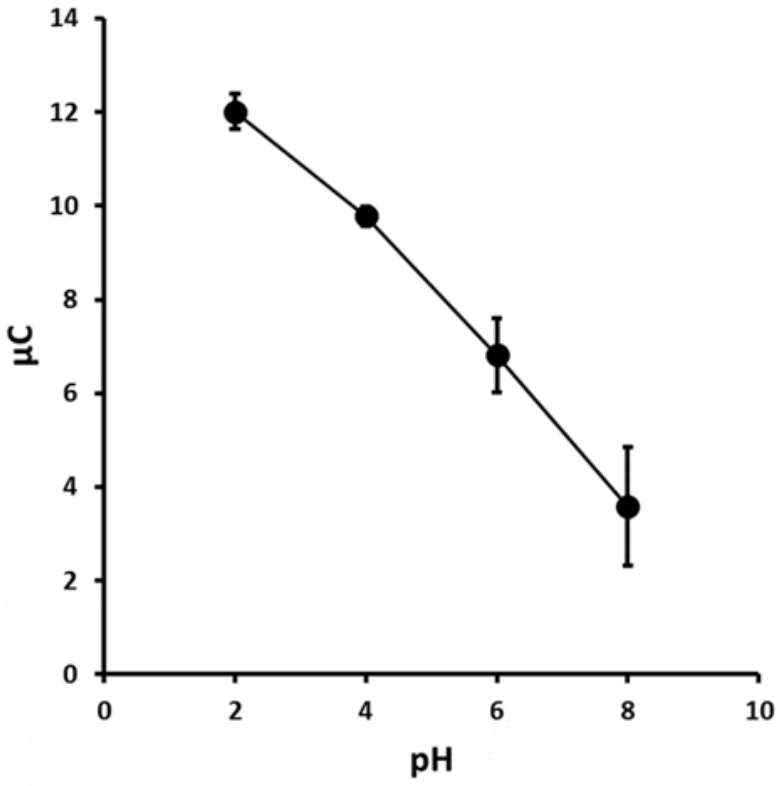

Figure 4. Chronoamperometric response versus pH for 1.0 mM 2,4-DNP. Each point is the mean of three separate measurements. Error bars represent ± σ.

3.5. Optimisation of Chronoamperometric Step Potentials

We first optimised the applied reduction potential used in the first step of the chronoamperometric measurement. The effect of this reduction potential was investigated over the range -0.4 V to -1.5 V by monitoring the resulting oxidation current recorded at +1.0 V (Figure 5). The oxidative chronoamperometric response was found to increase with increasing negative potential over the range -0.4 V to -0.9 V. At more negative potentials the oxidative response was found to reach a constant. However, as the potential beyond -1.0 V was made more negative the precision of the measurement improved with the lowest coefficient of variation (3.2 %) being obtained at -1.4 V. Consequently, an applied potential of -1.4 V was used for step 1 (reduction) of the chronoamperometric measurement in further studies.

We next investigated the oxidative measurement step (step 2). The effect of applied potential was studied over the range +0.2 V to +1.0 V. In this investigation, the resulting chronoamperometric signal was found to increase with increasing positive potential over the range +0.2 V to +0.8 V. The signal was found to become constant at more positive potentials and so further studies were undertaken using an applied step 2 potential of +0.8 V.

 doi:10.20944/preprints202505.0594.v1

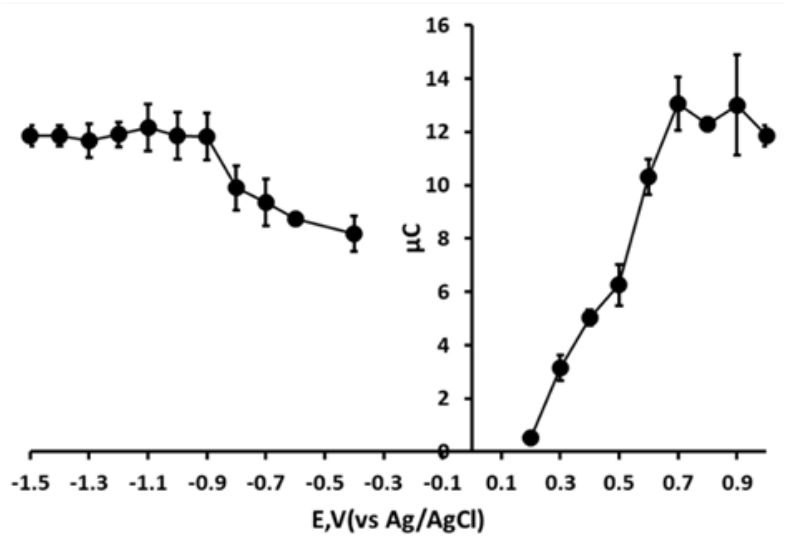

Figure 5. Effect of reduction and oxidation step potentials. Each point is the mean of three separate measurements. Error bars represent ± σ.

3.6. The Effect of Time on the Chronoamperometric Response

The effect of step 1 reduction time on the resulting oxidative chronoamperometric response was investigated over the range 10 s to 120 s. The response (oxidation signal) was found to increase with time, following a log relationship (Figure 6). In this proof-of-concept investigation based on a balance of time against sensitivity, a step 1 reduction time of 60 s was selected and used in further investigations.

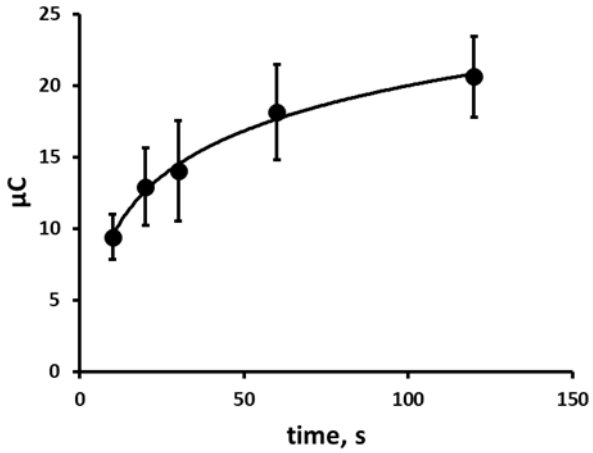

Figure 6. Effect of reduction step time on resulting chronoamperogram. Each point is the mean of three separate measurements. Error bars represent ± σ.

3.7. Calibration Curve and Limit of Detection

Initial studies were undertaken to study the effect of 2,4-DNP concentrations on the magnitude of the chronoamperometric response. The calibration plot was found to be linear from 50 µM to 1.0 mM (R^2 = 0.9978), with a detection limit of 7.8 µM (based on a signal-to-noise ratio of three).

3.8. Analytical Application

The optimised procedure was used to determine the concentration of 2,4-DNP in fortified and unfortified environmental pond water samples (typical amperograms shown in Figure 7). A mean recovery of 106 % was obtained with an associated coefficient of variation of 3.6 %. These results

 doi:10.20944/preprints202505.0594.v1

show that the optimised chronoamperometric method is capable of determining 2,4-DNP in environmental water samples.

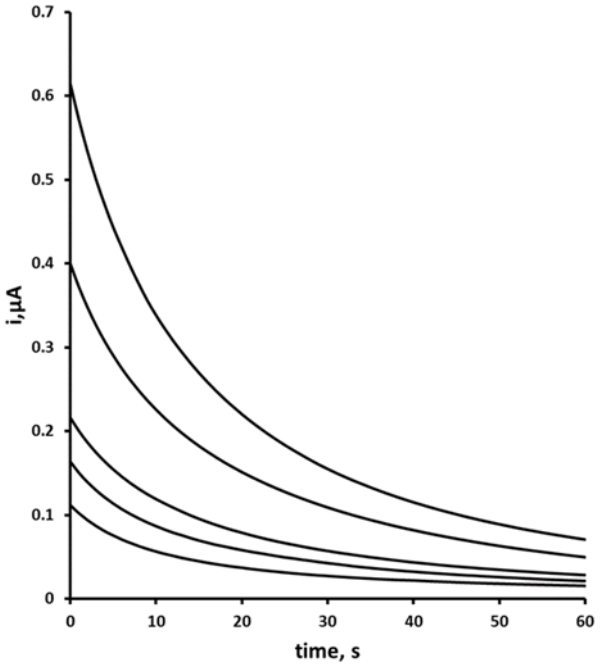

Figure 7. 2,4-DNP-fortified samples of an environmental water sample measured by double potential step chronoamperometry.

4. Conclusions

This is the first example of the voltammetric behaviour and chronoamperometric determination of 2,4-DNP at a fully 3D printed carbon nanofiber–graphite–polystyrene electrode. A simple double potential step chronoamperometric assay for 2,4-DNP was developed and well-defined amperometric signals can be obtained with a detection limit of 7.8 μM and a linear response from 50 μM up to 1.0 mM (R^2 = 0.9978). A mean recovery of 106 % (% CV = 3.6 %) was obtained for an environmental water sample fortified with 50 μM 2,4-DNP.

The results show that these 3D printed working electrodes can be utilised as viable alternatives to those fabricated from traditional materials and reliable data may be obtained for the determination of 2,4-DNP. The performance characteristics are similar to those previously reported at traditional electrode materials such as Hg modified Ag electrodes with detection limits ranging between 2.7 μM [57] to 10 μM [58] being reported. Notably, the detection limit is an improvement on that at Pt and Au electrodes of 85 μM [59]. A number of reports have shown that lower limits of detection can be obtained at carbon-based electrodes fabricated from more traditional materials such as glassy carbon. However, these have utilised secondary modifications to the electrode surface; including surfactants [60], graphene and molecularly printed polymers [61], metal nanoparticles [62], and sample preparation steps such as solid phase extraction [63] and liquid chromatography [64,65].

Author Contributions: Conceptualization, D.S.S. and K.C.H.; methodology, K.C.H; software, Z.R. and P.I.; validation, D.S.S. and K.C.H.; investigation, D.S.S. and K.C.H.; resources, K.C.H., Z.R. and P.I.; writing—original draft preparation, D.S.S. and K.C.H.; writing—review and editing, D.S.S. and K.C.H.; supervision, K.C.H.; project administration, K.C.H.; funding acquisition, K.C.H. All authors have read and agreed to the published version of the manuscript.

Funding: This research received no external funding.

Institutional Review Board Statement: Not applicable.

 doi:10.20944/preprints202505.0594.v1

Informed Consent Statement: Not applicable.

Data Availability Statement: Data will be made available on request.

Acknowledgments: The authors are grateful to the School of Applied Sciences, the Institute of Bio-Sensing Technology, University of the West of England, and the Department of Mechanical Engineering, University of Bath.

Conflicts of Interest: The authors declare no conflicts of interest.

Abbreviations

The following abbreviations are used in this manuscript:

Ag/AgCl	Silver/Silver Chloride
ATP	Adenosine Triphosphate
CAD	Computer-Aided Design
CV	Cyclic Voltammetry
2,4-DNP	2,4-Dinitrophenol
LC_{50}	Median Lethal Concentration

References

1. Dadban Shahamat, Y.; Sadeghi, M.; Shahryari, A.; Okhovat, N.; Bahrami Asl, F.; Baneshi, M.M. Heterogeneous catalytic ozonation of 2, 4-dinitrophenol in aqueous solution by magnetic carbonaceous nanocomposite: catalytic activity and mechanism, Desalination and Water Treatment 2016, 57, 20447-20456.
2. Nojima, K.; Kawaguchi, A.; Ohya, T.; Kanno, S.; Hirobe, M. Studies on photochemical reaction of air pollutants. X. Identification of nitrophenols in suspended particulates, Chemical and Pharmaceutical Bulletin 1983, 31, 1047-1051.
3. Callahan, M.A.; Slimak, M.W.; Gabel, N.W.; May, I.P.; Fowler, C.F.; Freed, J.R.; Jennings, P.; Durfee, R.L.; Whitmore, F.C.; Maestri, B.; Mabey, W.R.; Holt, B.R.; Gould, C. Water-Related Environmental Fate of 129 Priority Pollutants; Office of Water Planning and Standards, Office of Water and Waste Management, U.S. Environmental Protection Agency: Washington, D.C., 1979.
4. Dehghani, M.H.; Alghasi, A.; Porkar, G. Using medium pressure ultraviolet reactor for removing azo dyes in textile wastewater treatment plant, World Applied Sciences Journal 2011, 12, 797-802.
5. Paisio, C.E.; Agostini, E.; González, P.S.; Bertuzzi, M.L. Lethal and teratogenic effects of phenol on Bufo arenarum embryos, Journal of Hazardous Materials 2009, 167, 64-68.
6. Marit, J.S.; Weber, L.P. Acute exposure to 2, 4-dinitrophenol alters zebrafish swimming performance and whole body triglyceride levels, Comparative Biochemistry and Physiology Part C: Toxicology & Pharmacology 2011, 154, 14-18.
7. Kuzmina, V.V.; Tarleva, A.F.; Gracheva, E.L. Influence of various concentrations of phenol and its derivatives on the activity of fish intestinal peptidases, Inland Water Biology 2017, 10, 228-234.
8. Shea, P.J.; Weber, J.B.; Overcash, M.R. In Residue Reviews: Residues of Pesticides and Other Contaminants in the Total Environment; Gunther, F.A., Gunther, J.D., Eds.; Springer: New York, NY, USA, 1983; Volume 87, pp. 1-41.
9. Shaddad, M.A.; Radi, A.F.; El-Enany, A.E. Seed Germination, Transpiration Rate, and Growth Criteria as Affected by Various Concentrations of $CdCl_2$, NaF, and 2,4-DNP. Journal of Islamic Academy of Sciences, 1989, 2, 7-12.
10. Speer, H.L. The Effect of Arsenate and Other Inhibitors on Early Events during the Germination of Lettuce Seeds (Lactuca sativa L.), Plant Physiology 1973, 52, 142-146.
11. Wang, T.S.C.; Yang, T.-K.; Chuang, T.-T. Soil phenolic acids as plant growth inhibitors, Soil Science 1967, 103, 239-246.
12. Nanda, K.K.; Dhawan, A.K. A paradoxical effect of 2,4-dinitrophenol in stimulating the rooting of hypocotyl cuttings ofPhaseolus mungo, Experientia 1976, 32, 1167-1168.
13. Perkins, R.G. A study of the munitions intoxications in France, Public Health Reports 1919, 34, 2335-2374.

 doi:10.20944/preprints202505.0594.v1

14. Harris, M.O.; Corcoran, J. Toxicological Profile for Dinitrophenols; U.S. Department of Health and Human Services, United States Agency for Toxic Substances and Disease Registry: Washington, D.C., USA, 1995.
15. Hargreaves, I.P.; Al Shahrani, M.; Wainwright, L.; Heales, S.J.R. Drug-induced mitochondrial toxicity, Drug Safety 2016, 39, 661-674.
16. Boardman, W.W. Rapidly developing cataracts after dinitrophenol, California and Western Medicine 1935, 43, 118.
17. Petróczi, A.; Ocampo, J.A.V.; Shah, I.; Jenkinson, C.; New, R.; James, R.A.; Taylor, G.; Naughton, D.P. Russian roulette with unlicensed fat-burner drug 2,4-dinitrophenol (DNP): evidence from a multidisciplinary study of the internet, bodybuilding supplements and DNP users, Substance Abuse Treatment, Prevention, and Policy 2015, 10, 1-21.
18. Fernardes, V.F.; Izidoro, L.F.M. The Risks of Using 2,4-Dinitrophenol (2,4-DNP) as a Weight Loss Agent: A Literature Review , Annals of Clinical and Medical Case Reports 2022, 9, 1-7.
19. Freeman, N.; Moir, D.; Lowis, E.; Tam, E. 2, 4-Dinitrophenol:'diet'drug death following major trauma, Anaesthesia Reports 2021, 9, 106-109.
20. Abdelati, A.; Burns, M.M.; Chary, M. Sublethal toxicities of 2, 4-dinitrophenol as inferred from online self-reports, PLoS One 2023, 18, e0290630.
21. Rudenko, I.B.; Shaimardanova, D.R.; Kayumova, R.R. Clinical case report of acute dinitrophenol poisoning with a fatal outcome of Udmurt Republic, Sudebno-meditsinskaia Ekspertiza 2023, 66, 59-61.
22. Tuğcan, M.O.; Kekeç, Z. A Case of Fatal Poisoning: Use of 2-4 Dinitrophenol for Weight Loss, Anatolian Journal of Emergency Medicine 2024, 7, 87-90.
23. Mwesigwa, J.; Collins, D.J.; Volkov, A.G. Electrochemical signaling in green plants: effects of 2, 4-dinitrophenol on variation and action potentials in soybean, Bioelectrochemistry 2000, 51, 201-205.
24. Geisler, J.G.; Marosi, K.; Halpern, J.; Mattson, M.P. DNP, mitochondrial uncoupling, and neuroprotection: A little dab'll do ya, Alzheimer's & Dementia 2017, 13, 582-591.
25. Lee, Y.; Heo, G.; Lee, K.M.; Kim, A.H.; Chung, K.W.; Im, E.; Chung, H.Y.; Lee, J. Neuroprotective effects of 2, 4-dinitrophenol in an acute model of Parkinson's disease, Brain Research 2017, 1663, 184-193.
26. Wu, B.; Jiang, M.; Peng, Q.; Li, G.; Hou, Z.; Milne, G.L.; Mori, S.; Alonso, R.; Geisler, J.G.; Duan, W. 2, 4 DNP improves motor function, preserves medium spiny neuronal identity, and reduces oxidative stress in a mouse model of Huntington's disease, Experimental Neurology 2017, 293, 83-90.
27. Perry, R.J.; Zhang, D.; Zhang, X.-M.; Boyer, J.L.; Shulman, G.I. Controlled-release mitochondrial protonophore reverses diabetes and steatohepatitis in rats, Science 2015, 347, 1253-1256.
28. Honeychurch, K.C.; Brooks, J.; Hart, J.P. Development of a voltammetric assay, using screen-printed electrodes, for clonazepam and its application to beverage and serum samples, Talanta 2016, 147, 510-515.
29. Honeychurch, K.C.; Davidson, G.M.; Brown, E.; Hart, J.P. Novel reductive–reductive mode electrochemical detection of Rohypnol following liquid chromatography and its determination in coffee, Analytica Chimica Acta 2015, 853, 222-227.
30. Honeychurch, K.C.; Smith, G.C.; Hart, J.P. Voltammetric behavior of nitrazepam and its determination in serum using liquid chromatography with redox mode dual-electrode detection, Analytical Chemistry 2006, 78, 416-423.
31. Honeychurch, K.C. Development of an electrochemical assay for the illegal “fat burner” 2, 4-dinitrophenol and its potential application in forensic and biomedical analysis, Advances in Analytical Chemistry 2016, 6, 41-48.
32. Xu, F.; Guan, W.; Yao, G.; Guan, Y. Fast temperature programming on a stainless-steel narrow-bore capillary column by direct resistive heating for fast gas chromatography, Journal of Chromatography A 2008, 1186, 183-188.
33. Preiss, A.; Bauer, A.; Berstermann, H.-M.; Gerling, S.; Haas, R.; Joos, A.; Lehmann, A.; Schmalz, L.; Steinbach, K. Advanced high-performance liquid chromatography method for highly polar nitroaromatic compounds in ground water samples from ammunition waste sites, Journal of Chromatography A 2009, 1216, 4968-4975.
34. Xu, L.; Huang, Y.; Zhao, B.; Ren, L.; Long, T. Determination of 2, 4-Dichlorophenol, 2, 4-Dinitrophenol, and Bisphenol a in River Water by Magnetic Solid-Phase Extraction (MSPE) Using β-Cyclodextrin Modified

 doi:10.20944/preprints202505.0594.v1

Magnetic Ferrite Microspheres and High-Performance Liquid Chromatography – Diode Array Detection (HPLC-DAD), Analytical Letters 2022, 55, 367-377.

35. Hofmann, D.; Hartmann, F.; Herrmann, H. Analysis of nitrophenols in cloud water with a miniaturized light-phase rotary perforator and HPLC-MS, Analytical and Bioanalytical Chemistry 2008, 391, 161-169.
36. Gross, B.; Lockwood, S.Y.; Spence, D.M. Recent advances in analytical chemistry by 3D printing, Analytical Chemistry 2017, 89, 57-70.
37. . Pan, L.; Shijing, Z.; Yang, J.; Fei, T.; Mao, S.; Fu, L.; Lin, C.T. 3D-Printed Electrodes for Electrochemical Detection of Environmental Analytes. Anal. Methods 2025, 17, 2235–2253.
38. . Selemani, M.A.; Cenhrang, K.; Azibere, S.; Singhateh, M.; Martin, R.S. 3D Printed Microfluidic Devices with Electrodes for Electrochemical Analysis. Anal. Methods 2025, 17, 2235–2253.
39. . Crapnell, R.D.; Banks, C.E. Electroanalysis Overview: Additive Manufactured Biosensors Using Fused Filament Fabrication. Anal. Methods 2024, 16, 2625–2634.
40. Su, C.-K.; Peng, P.-J.; Sun, Y.-C. Fully 3D-printed preconcentrator for selective extraction of trace elements in seawater, Analytical Chemistry 2015, 87, 6945-6950.
41. Jones, R.; Haufe, P.; Sells, E.; Iravani, P.; Olliver, V.; Palmer, C.; Bowyer, A. RepRap–the replicating rapid prototype, Robotica 2011, 29, 177-191.
42. Kitson, P.J.; Glatzel, S.; Chen, W.; Lin, C.-G.; Song, Y.-F.; Cronin, L. 3D printing of versatile reactionware for chemical synthesis, Nature Protocols 2016, 11, 920-936.
43. Ambrosi, A.; Pumera, M. 3D-printing technologies for electrochemical applications, Chemical Society Reviews 2016, 45, 2740-2755.
44. Djafari, Y.; Abolfathi, N. An inexpensive 3D printed amperometric oxygen sensor for transcutaneous oxygen monitoring, 2016 23rd Iranian Conference on Biomedical Engineering and 2016 1st International Iranian Conference on Biomedical Engineering (ICBME) 2016, 281-284.
45. Honeychurch, K.C.; Rymansaib, Z.; Iravani, P. Anodic stripping voltammetric determination of zinc at a 3-D printed carbon nanofiber–graphite–polystyrene electrode using a carbon pseudo-reference electrode, Sensors and Actuators B: Chemical 2018, 267, 476-482.
46. Loo, A.H.; Chua, C.K.; Pumera, M. DNA biosensing with 3D printing technology, Analyst 2017, 142, 279-283.
47. Pohanka, M. Three-dimensional printing in analytical chemistry: principles and applications, Analytical Letters 2016, 49, 2865-2882.
48. Ragones, H.; Schreiber, D.; Inberg, A.; Berkh, O.; Kósa, G.; Freeman, A.; Shacham-Diamand, Y. Disposable electrochemical sensor prepared using 3D printing for cell and tissue diagnostics, Sensors and Actuators B: Chemical 2015, 216, 434-442.
49. Rymansaib, Z.; Iravani, P.; Emslie, E.; Medvidović-Kosanović, M.; Sak-Bosnar, M.; Verdejo, R.; Marken, F. All-polystyrene 3D-printed electrochemical device with embedded carbon nanofiber-graphite-polystyrene composite conductor, Electroanalysis 2016, 28, 1517-1523.
50. Salvo, P.; Raedt, R.; Carrette, E.; Schaubroeck, D.; Vanfleteren, J.; Cardon, L. A 3D printed dry electrode for ECG/EEG recording, Sensors and Actuators A: Physical 2012, 174, 96-102.
51. Silva, M.V.C.O.; Carvalho, M.S.; Silva, L.R.G.; Rocha, R.G.; Cambraia, L.V.; Janegitz, B.C.; Nossol, E.; Muñoz, R.A.A.; Richter, E.M.; Stefano, J.S. Tailoring 3D-Printed Sensor Properties with Reduced-Graphene Oxide: Improved Conductive Filaments. Microchimica Acta 2024, 191, 633.
52. Brum, R.R.D.; de Faria, L.V.; Caldas, N.M.; Pereira, R.P.; Peixoto, D.A.; Silva, S.C.; Nossol, E.; Semaan, F.S.; Pacheco, W.F.; Rocha, D.P.; Dornellas, R.M. 3D-Printed Electrochemical Sensor Based on Graphite-Alumina Composites: A Sensitive and Reusable Platform for Self-Sampling and Detection of 2,4,6-Trinitrotoluene Residues in Environmental and Forensic Applications. Talanta Open 2025, 11, 100441.
53. Wang, Z.; Zhan, Z.; Liu, Y.; Fan, F.; Li, S.; Song, Z.; Yang, W.; Duan, H.; Cui, S.; He, X. An Intelligent Portable Point-of-Care Testing (POCT) Device for On-Site Quantitative Detection of TNT Explosive in Environmental Samples. Sensors and Actuators B: Chemical, 2025, 439, 137846.
54. Pearce, P.J.; Simkins, R.J.J. Acid strengths of some substituted picric acids, Canadian Journal of Chemistry 1968, 46, 241-248.

 doi:10.20944/preprints202505.0594.v1

55. Yin, H.; Zhou, Y.; Han, R.; Qiu, Y.; Ai, S.; Zhu, L. Electrochemical oxidation behavior of 2, 4-dinitrophenol at hydroxylapatite film-modified glassy carbon electrode and its determination in water samples, Journal of Solid State Electrochemistry 2012, 16, 75-82.
56. Pletcher, D.; Greff, R.; Peat, R.; Peter, L.M.; Robinson, J. Instrumental Methods in Electrochemistry; Elsevier, 2001.
57. Fischer, J.; Vanourkova, L.; Danhel, A.; Vyskocil, V.; Cizek, K.; Barek, J.; Peckova, K.; Yosypchuk, B.; Navratil, T. Voltammetric determination of nitrophenols at a silver solid amalgam electrode, International Journal of Electrochemical Science 2007, 2, 226-234.
58. Danhel, A.; Shiu, K.K.; Yosypchuk, B.; Barek, J.; Peckova, K.; Vyskocil, V. The use of silver solid amalgam working electrode for determination of nitrophenols by HPLC with electrochemical detection, Electroanalysis 2009, 21, 303-308.
59. Khachatryan, K.S.; Smirnova, S.V.; Torocheshnikova, I.I.; Shvedene, N.V.; Formanovsky, A.A.; Pletnev, I.V. Solvent extraction and extraction–voltammetric determination of phenols using room temperature ionic liquid, Analytical and Bioanalytical Chemistry 2005, 381, 464-470.
60. Wang, X.-G.; Wu, Q.-S.; Liu, W.-Z.; Ding, Y.-P. Simultaneous determination of dinitrophenol isomers with electrochemical method enhanced by surfactant and their mechanisms research, Electrochimica Acta 2006, 52, 589-594.
61. Liu, Y.; Zhu, L.; Zhang, Y.; Tang, H. Electrochemical sensoring of 2, 4-dinitrophenol by using composites of graphene oxide with surface molecular imprinted polymer, Sensors and Actuators B: Chemical 2012, 171, 1151-1158.
62. Yang, P.; Cai, H.; Liu, S.; Wan, Q.; Wang, X.; Yang, N. Electrochemical reduction of 2, 4-dinitrophenol on nanocomposite electrodes modified with mesoporous silica and poly (vitamin B1) films, Electrochimica Acta 2011, 56, 7097-7103.
63. Lezi, N.; Economou, A.; Barek, J.; Prodromidis, M. Screen-Printed Disposable Sensors Modified with Bismuth Precursors for Rapid Voltammetric Determination of 3 Ecotoxic Nitrophenols, Electroanalysis 2014, 26, 766-775.
64. Karaová, J.; Barek, J.; Schwarzová-Pecková, K. Oxidative and Reductive Detection Modes for Determination of Nitrophenols by High-Performance Liquid Chromatography with Amperometric Detection at a Boron Doped Diamond Electrode, Analytical Letters 2016, *49*, 66-79.
65. Ruana, J.; Urbe, I.; Borrull, F. Determination of phenols at the ng/l level in drinking and river waters by liquid chromatography with UV and electrochemical detection, Journal of Chromatography A 1993, *655*, 217-226.